Oxidation of SO_2 and formation of water droplets under irradiation of 20MeV protons in $N_2/H_2O/SO_2$

Tomita, Shigeo; Nakai, Yoichi; Funada, Shuhei; Tanikawa, Hideomi; Harayama, Isao; Kobara, Hitomi; Sasa, Kimikazu; Pedersen, Jens Olaf Pepke; Hvelplund, Preben

Published in:
Nuclear Instruments and Methods in Physics Research Section B: Beam Interactions with Materials and Atoms

Link to article, DOI:
10.1016/j.nimb.2015.08.073

Publication date:
2015

Document Version
Peer reviewed version

Oxidation of SO_2 and Formation of Water Droplets under Irradiation of 20 MeV protons in $N_2/H_2O/SO_2$

Shigeo Tomita[a], Yoichi Nakai[b,*], Shuhei Funada[a], Hideomi Tanikawa[a], Isao Harayama[a], Hitomi Kobara[c], Kimikazu Sasa[d], Jens Olaf Pepke Pedersen[e], Preben Hvelplund[f]

[a] *Institute of Applied Physics, University of Tsukuba, Tsukuba, Ibaraki 305-8573, Japan*

[b] *RIKEN Nishina Center, Radioactive Isotope Laboratory, Wako, Saitama 351-0198, Japan*

[c] *National Institute of Advanced Industrial Science and Technology, Tsukuba, Ibaraki 305-8569, Japan*

[d] *Tandem Accelerator Complex, University of Tsukuba, Tsukuba, Ibaraki 305-8577, Japan*

[e] *National Space Institute, Technical University of Denmark, DK-2800 Kgs. Lyngby, Denmark*

[f] *Department of Physics and Astronomy, University of Aarhus, DK-8000 Aarhus, Denmark*

Abstract

We have performed an experiment on charged droplet formation in a humidified N_2 gas with trace SO_2 concentrations and induced by 20 MeV proton irradiation. It is thought that SO_2 reacts with the chemical species, such as OH radicals, generated through the reactions triggered by N_2^+ production. Both droplet number and droplet size increased with SO_2 consumption for the proton irradiation. The total charged droplet numbers entering the differential mobility analyzer per unit time were proportional to the 0.68 power of the SO_2 consumption. These two findings suggest that coagulation among the small droplets contributes to the formation of the droplets. The charged droplet volume detected per unit time is proportional to the SO_2 consumption, which indicates that a constant amount of sulfur atoms is contained in a unit volume of droplet, regardless of different droplet-size distributions depending on the SO_2 consumption.

Keywords:

nanoparticle formation, sulfur dioxide, fast ion irradiation

* corresponding author : nakaiy@riken.jp

1. Introduction

Gas-phase particle formation induced by ionization processes (ion-induced nucleation) has been studied for decades and is a well-known mechanism in cloud chambers. In the last two decades, since the correlation of galactic cosmic rays (GCRs) with the coverage of clouds in the low troposphere was reported [1,2], ion-induced nucleation in the air has attracted attention as one of mechanisms in cloud particle formation. The cloud particle formation by GCRs is generally explained as follows: 1) the GCRs ionize molecules in the air, 2) the primary ions interact with molecules in the air and may form ionic clusters, 3) the ionic clusters can grow and pass the critical size of particle formation through attachment of molecules due to their stability caused by attractive polarization forces by an ion charge. As mentioned above, ion-induced nucleation has been also considered as one of important pathways for particle formation in the atmosphere [3,4].

Many laboratory investigations for particle (droplet) formation have been performed using a variety of ionizing methods [5-18]. Imanaka *et al*. [10] performed charged droplet formation

(about 10 nm diameter) in non-saturated humidified nitrogen gas (without trace components) using an intense 20 MeV proton beam. However, most of studies were carried out using air with trace gas components, such as sulfuric acid, ammonia, and so on. These trace components are thought to contribute to the enhancement of the droplet formation. Sulfuric acid generated by SO_2 oxidation decreases the free-energy barrier of the droplet growth in the binary nucleation process of water and sulfuric acid [19]. Under particle irradiation, the droplet formation is further enhanced in the gas with trace components. For instance, the experiment using high-energy electrons suggests that the droplet formation under the irradiation of ionizing particles is clearly contributed from ion-induced nucleation [7]. The difference from a theoretical model was found in other experiment, where it was pointed out that the difference might be attributed to the oxidation of SO_2 induced by the ionizing radiations [9,13,20].

Recently, the CLOUD project at CERN has performed large-scale experiments for confirming the role of ion-induced nucleation using a high-energy pion beam and a 27 m^3 cloud chamber with a large number of analyzing instruments. Their results revealed that ion induced nucleation occurs for all temperatures, humidities and cluster compositions observed, but has a minor importance in the atmospheric boundary layer. Amines, ammonia and sulfur dioxide was found to enhance nucleation rates under a broad range of conditions representative of the boundary layer [8,15]. However, in clean environments, such as the terrestrial middle atmosphere, ion-induced nucleation may account for more than half of the

nucleation rate [14].

In the present study, we performed a measurement of the size distributions of the charged droplets produced by 20 MeV proton irradiation of a mixed gas of pure nitrogen, water vapor and sulfur dioxide while monitoring the concentration of sulfur dioxide. Note that sulfuric acid, H_2SO_4, itself was not prepared in the sample gas. In the following, we will discuss the relation of the SO_2 consumption with the proton beam intensity and the SO_2 concentration. Moreover, the size distributions, the particle-flow rate and the volume-yield rate for the produced droplets will be discussed.

2. Experiments

The experiments on proton irradiation were conducted on the Tandem Accelerator (12UD Pelletron) at the Tandem Accelerator Complex, University of Tsukuba (UTTAC). A schematic drawing of the present experimental setup is shown in fig. 1, which is similar to the previous experiment performed by Imanaka *et al* [10]. The present setup consists of a humidified gas generator, an irradiation chamber for the proton beam, a differential mobility analyzer (DMA) for particle size analysis, and a monitor of the SO_2 concentration. A humidified nitrogen gas was generated by bubbling ultra-pure water (18.2 MΩcm in electrical resistivity) with pure nitrogen (99.9995%). The humidified gas was subsequently mixed with a dry nitrogen gas with the same purity. The humidity of the sample gas was adjusted by controlling the flow rates of the wet and dry gases. After mixing wet and dry nitrogen gases, an SO_2/N_2 gas (with a

SO_2 mixing ratio of 20 ppm) was added to the gas flow. The total flow rate of the sample gas was kept at 2 SLM (Standard Liters per Minute).

The sample gas was introduced into the irradiation chamber constructed from a stainless-steel cross tube with a volume of 227 cm^3. The residence time of the introduced gas was 6.8 sec. The relative humidity and temperature of the gas in the irradiation chamber were monitored using a hygrometer with accuracies ±0.2°C and ±1.0% for temperature and relative humidity, respectively.

The 20 MeV proton beam delivered from the accelerator crossed the flow of sample gas at a right angle through polyimide-film windows of 7.5 μm thickness. The beam current was monitored with a Faraday cup located downstream of the irradiation chamber. The energy loss of a 20 MeV proton in the polyimide foils was negligibly small (25 keV according to SRIM code [21]). Under the assumptions that primary ions originate from N_2, the ionization rate is estimated to be about 1.4×10^{13} pairs/sec for a proton beam current of 200 pA, using the energy deposit in the irradiation chamber (about 370 keV per one proton in nitrogen gas) and the average energy of 34.5 eV/pair for production of a ion-electron pair [22]. Most of the positive and negative species (electrons and negative ions) recombine in a short time, where other ion-molecule reactions competitively occur. Consequently, ionization and recombination are almost in equilibrium. The total ion density in the irradiation area was roughly estimated to be in the order of 10^9 cm^{-3} for 200 pA proton beam with a typical beam diameter of 5 mm and the path length of 130 mm in the gas, if the equilibrium between ionization and

recombination for positive ions and negatively charged species is achieved in the irradiation area, taking account of the fact that the recombination coefficient is in the order of 10^{-6} cm^3/sec [23]. Note that, as mentioned above, the recombination and ion-molecule reactions simultaneously proceed, but that the total ion density is controlled by the rates of ionization and recombination processes. Furthermore, ions are neutralized due to recombination out of the irradiation area.

After irradiation by protons, the sample gas was transported into the DMA, in which the electrical mobility distribution of the charged droplets in the sample gas was measured [24,25]. The electrical mobility was converted to the droplet size using the Stokes-Cunningham formula under the assumption that the charge on a droplet was unity [10,16]. Furthermore, SO_2-concentration variation between beam-on and off (SO_2 consumption) was measured using a SO_2 analyzer based on ultra-violet fluorescence (Thermo 43S). The path of gas flow downstream of the irradiation chamber could be switched to either droplet size analysis or measurement of the SO_2-concentration variation.

For comparison with the proton irradiation, a positive corona discharge in the irradiation chamber was also employed, where the DC voltage applied to a needle was a few kV.

3. Results and discussion

Figure 2 shows SO_2 consumption versus the proton-beam current. As a result of fitting the data points using a power function, it is found that the SO_2 consumption is not proportional to

beam current but to the 0.67 power of the beam current. This indicates that the contribution from direct dissociation and ionization of SO_2 by protons is small. SO_2 is presumably consumed by produced ions, electrons, or radicals from nitrogen and/or H_2O, considering that these reactive products by proton irradiation rapidly decrease through ion-electron/ion-ion recombination and radical-radical reactions and that their densities consequently are not proportional to the beam current.

In fig. 2, the SO_2 consumptions are also shown for different humidities (9% and 52%) at a beam current close to 200 pA. No clear dependence on humidity is seen. It does not imply, at least, that the radicals produced in H_2O dissociation directly participate in the first-stage reactions related with the SO_2 consumption. Thus, it can be assumed that positive ions, electrons, or negative ions produced by proton irradiation plays important roles for the SO_2 consumption.

It is known that ionization processes cause the reaction of $SO_2+O_3^- \rightarrow SO_3^-+O_2$ in air containing SO_2 [17,26,27]. Enghoff et al. [13] also indicated that this reaction is important in sulfuric acid production from SO_2 induced by ionizing processes without photochemical reactions. However, the production of O_3^- should be suppressed because no O_2 was mixed in the present sample gas and O_3^- should be produced from the reactions containing H_2O. Therefore, it is thought that the OH radical becomes a significant chemical species: the SO_2 is consumed through an attachment of OH on SO_2 as photochemical oxidation of SO_2 and eventually sulfuric acid is generated [28]. Taking into account the densities of nitrogen and

water, many of the produced OH radicals are considered to originate not from the direct dissociation of H_2O but from rapid ion-reaction chains such as $N_2^+ + H_2O \rightarrow N_2 + H_2O^+$ and $H_2O^+ + H_2O \rightarrow H_3O^+ + OH$ [29], where these ion-molecule reactions and the recombination processes proceed simultaneously and competitively, as mentioned above. The recombination between H_2O^+ ions and electrons is also considered to produce OH radicals [29]. The above finding that SO_2 consumptions were almost independent of humidity supports this speculation since H_2O molecules are much more numerous than N_2^+ (and electrons) in the present conditions. It is also reasonable to assume that the OH production is not proportional to the beam current since it is affected by a complicated reaction network including ion-electron/ion-ion recombination and reactions among chemical species produced by proton irradiation.

In fig. 3, the relation of the SO_2 consumption with the SO_2 concentration (mixing ratio) is shown for a 200 pA proton beam and a humidity of 30% RH. The SO_2 consumption is approximately proportional to the SO_2 concentration. It means that SO_2 participates only once in the reactions associated with the SO_2 consumption. Thus, most products of the SO_2 consumption reactions are thought to contain only one sulfur atom. In the present study, the SO_2 consumption was adjusted by two ways: changing beam current and changing SO_2 concentration.

Figure 4 shows mobility distributions of positively and negatively charged droplets produced by irradiation of a 200 pA proton beam into a humidified gas of 30% RH for several

SO_2 concentrations (20 ppb or higher). Not only the number of the droplets but also their size increase with the SO_2 concentration. This indicates that the droplet production and growth becomes faster with increasing SO_2 consumption, considering the proportional relation between of SO_2 concentration and consumption. Mobility distributions of both positively and negatively charged species are almost equivalent and have a peak distribution around 10 nm diameter. The equivalence stems from the fact that the droplets are charged by bipolar ions. Under bipolar charging, the average charged fraction (both positive and negative) was less than 0.1 for the droplets having a diameter of 10 nm, and thus the charge on the droplets is unity. Furthermore, it must be mentioned that there is almost 10 times higher concentration of neutral droplets [16]. The distributions for positively charged droplets at low SO_2 concentrations exhibit another small peak in the region of diameters less than 3 nm corresponding to a mobility of a few $cm^2V^{-1}s^{-1}$. The region of mobility is in the same order as the polarization limit of charged particles in N_2 gas. Thus, the peak corresponds to small ions such as small $H_3O^+(H_2O)_n$ and/or $NH_4^+(H_2O)_n$ clusters which do not attach to the nanoparticle. This agrees reasonably with the fact that the peak appears only when the nanoparticle yield is low.

Figure 5 shows mobility distributions of positively charged droplets produced by corona discharge in a humidified gas of 30% RH with several SO_2 concentrations (50 ppb or higher). The SO_2 consumptions were 1.6, 3.6, 5.1, and 8.1 ppb corresponding to the SO_2 concentration of 40, 100, 150, and 200 ppb, respectively. It is noteworthy that the distributions have a single

peak in the region of diameters larger than 3 nm, i.e., the droplets larger than ionic cluster region were produced even by positive corona discharge. This is quite different from the case of humidified nitrogen gas without trace SO_2 gas, where only a single peak corresponding to small ions was observed [10]. Considering the fact that the SO_2 consumptions by the present corona discharge experiment were as large as with proton irradiation, this difference indicates that chemical species formed through reactions involving SO_2, such as sulfuric acid, has a crucial role even for positively charged droplet formation in the present case. Nagato and Nakauchi [18] found that the positive corona discharge generated none or only slight droplets in the humidified air involving 20 ppb SO_2 but that more droplet formation occurred by negative corona discharge at the same SO_2 concentration, although their sample gas contains trace ammonia. They also found that the positive ionic clusters generated in a positive corona discharge contain little sulfuric acid. Hvelplund et al. [30] observed the protonated ionic clusters containing sulfuric acid using discharge ionization but their intensities were low even for high mixing ratio of SO_2 (1%). Therefore, it is supposed that the positive ionic clusters rarely include sulfuric acid at low SO_2 concentrations and that the SO_2 consumption contributes little to the direct formation of the positively charge droplets from positive ionic clusters, i.e., the existence of other mechanisms on positive droplet formation is suggested.

Nagato and Nakauchi [18] revealed that the recombination between positively and negatively charged species strongly enhances droplet formation even with trace amounts of SO_2. In the present case, the distributions for the proton irradiation shift to larger size than for

corona discharge. This maybe reflects an effect of the recombination.

Particle-flow rates of positively charged droplets measured using the DMA are shown as a function of SO_2 consumption in fig. 6. The measurement using N_2/H_2O gas with 73% RH is also plotted as a reference for zero SO_2 consumption. The charge on each droplet was assumed to be unity. The data with both ways of adjusting SO_2 consumption are plotted in the same figure (see the figure caption). A clear difference cannot be seen within the uncertainties of the SO_2 consumption. The particle-flow rates are not thought to be proportional to the SO_2 consumption. The reference data at zero SO_2 consumption is negligibly small compared with the present data. Thus, we obtain the relation of $R \propto S^{0.68}$, where R is a particle-flow rate and S the SO_2 consumption. This non-linear relation is presumably associated with the fact that both the density and the size of droplets increase with increasing the SO_2 consumption as shown in fig.4. It implies that particle-size growth occurs rapidly due to coagulation of smaller droplets with increasing droplet density. Consequently, an increase of the particle-flow rate becomes slower with droplet density. Kobara *et al*. [31] observed particle-size growth in the region of 10 nm diameter due to coagulation in their experiment for particle generation by SO_2 gas-to-particle conversion through photochemical reactions. If we suppose that particle-size growth in the 10 nm region is mainly caused by coagulation of smaller particles, the reason for the difference of the diameter distributions between proton irradiation and positive corona discharge can be considered to be the enhancement of the particle formation due to ion-ion recombination as pointed out by Nagato and Nakauchi [18],

i.e., the particle density increases because of ion-ion recombination and, consequently, the sizes of particles grow due to their coagulation. Note that a number of neutral particles are also considered to be produced by proton irradiation, through the fact that small charged fraction (less than 0.1) is obtained for droplets with diameters less than 10 nm [10,16]. Thus, the coagulation between a charged particle and a neutral particle is supposed to dominantly cause the size growth.

Volume-yield rates of positively charged droplets are shown as a function of SO_2 consumption in fig. 7. The volume-yield rate corresponds to the droplet volume detected per unit time with the DMA. It was estimated by considering the mobility distributions represented as a function of droplet diameter, where we assumed unity charge per a droplet. The measurement using N_2/H_2O gas with 73% RH is also plotted as a reference data point for zero SO_2 consumption and it is negligibly small compared with the present results. The volume-yield rate is almost proportional to the SO_2 consumption and this indicates that a constant amount of sulfur atoms is contained in a unit volume of droplet, regardless of the mean droplet size, where the main carrier of sulfur atoms is probably sulfuric acid.

The proportional relation of the volume-yield rate with the SO_2 consumption shown in fig.7 provides an amount of consumed sulfur atoms per unit volume-yield rate of positively charged droplets: $\sim 1\times10^{23}$ atoms are consumed for a volume-yield rate of 1 cm^3/sec for positively charged droplets. Taking into account almost equivalent mobility distributions of positively and negatively charged droplets and the charging fraction of droplets with ~10 nm

diameter, which is supposed to be about 5% for both of positive and negative droplets (see experiments on bipolar diffusion charging [16]), around 5×10^{21} sulfur atoms are consumed for a total volume-yield rate of 1 cm^3/sec for neutral and charged particles. Since ~3×10^{22} water molecules are contained in 1 cm^3 liquid water, the fraction of contained sulfuric compounds, probably sulfuric acid, are crudely estimated to be ~15% or less of the number of other molecules in the droplets.

4. Summary

We have performed an experimental investigation for the charged droplet formation in a humidified N_2 gas with trace of SO_2 induced by 20 MeV proton irradiation, where the SO_2 consumption is also measured. The SO_2 consumption is controlled by the concentrations of the chemical species, such as OH radicals, generated through the ion-molecule reactions triggered by N_2^+ production. This consumption is approximately proportional to the 0.67 power of the beam current, but also approximately proportional to the SO_2 concentration, which implies that SO_2 participates only once in the reaction chain related to the SO_2 consumption.

The droplet size distributions converted from the mobility distributions are obtained in the proton irradiation. Both droplet number and droplet size increase with the SO_2 concentration, i.e., the SO_2 consumption. The particle-flow rates, total numbers of positively or negatively charged particles entering the DMA per unit time, are proportional to the 0.68 power of the

SO_2 consumption. These two findings for the dependences of the droplet-size distributions and the particle-flow rates on the SO_2 consumption suggest that coagulation among the small droplets [31] contributes to the formation of the droplets in the region of 10 nm diameter.

We also performed a measurement of positively charged droplets formed using positive corona discharge. In this case, the droplets larger than 3 nm are observed only with SO_2. This implies that SO_2 plays a crucial role for the droplet formation. However, when considering other investigations for droplet formation using corona discharge [18,30], the positive ionic clusters are thought to rarely include sulfuric acid at low SO_2 concentrations. Thus, it is supposed that the SO_2 does probably not contribute to direct droplet formation from positive ionic clusters. In addition, the difference between the size distributions for the proton irradiation and the positive corona discharge may reflect an enhancement of the particle formation by ion-ion recombination [18].

The volume-yield rates, the charged-droplet volumes detected per unit time, are proportional to the SO_2 consumption. It indicates that a constant amount of sulfur atoms is contained in a unit volume of droplets, regardless of droplet size distribution. The proportional relation shows that the number fraction of contained sulfuric compounds are crudely ~15% or less of other molecules in the droplets.

Acknowledgments

The authors would like to thank Prof. Kenkichi Nagato at National Institute of Technology,

Kochi College for his helpful discussion. This work was supported by JSPS Grants-in-Aid for Scientific Research (Grant Number: 23540462). One of author (Y. N.) also acknowledges for the partial support by JSPS Grants-in-Aid for Scientific Research (Grant Number: 25287148).

References

[1] H. Svensmark and E. FriisChristensen, Journal of Atmospheric and Solar-Terrestrial Physics **59**, 1225 (1997).

[2] N. D. Marsh and H. Svensmark, Phys. Rev. Lett. **85**, 5004 (2000).

[3] J. Curtius, E. R. Lovejoy, and K. D. Froyd, Space Science Reviews **125**, 159 (2006).

[4] F. Arnold, Space Science Reviews **137**, 225 (2008).

[5] K. G. Vohra, M. C. S. Ramu, and T. S. Muraleedharan, Atmos. Environ. **18**, 1653 (1984).

[6] J. Duplissy *et al.*, Atmos. Chem. Phys. **10**, 1635 (2010).

[7] M. B. Enghoff, J. O. Pepke Pedersen, U. I. Uggerhøj, S. M. Paling, and H. Svensmark, Geophys. Res. Lett. **38**, L09805 (2011).

[8] J. Kirkby *et al.*, Nature **476**, 429 (2011).

[9] H. Svensmark, M. B. Enghoff, and J. O. P. Pedersen, Phys. Lett. A **377**, 2343 (2013).

[10] M. Imanaka, S. Tomita, S. Kanda, M. Fujieda, K. Sasa, J. Olaf Pepke Pedersen, and H. Kudo, J. Aerosol Sci **41**, 468 (2010).

[11] T. Hakoda, H.-H. Kim, K. Okuyama, and T. Kojima, J. Aerosol Sci **34**, 977 (2003).

[12] K. Nagato, C. S. Kim, M. Adachi, and K. Okuyama, J. Aerosol Sci **36**, 1036 (2005).

[13] M. B. Enghoff *et al.*, Atmospheric Chemistry and Physics **12**, 5319 (2012).

[14] M. B. Enghoff, J. O. P. Pedersen, T. Bondo, M. S. Johnson, S. Paling, and H. Svensmark, J. Phys. Chem. A **112**, 10305 (2008).

[15] J. Almeida *et al.*, Nature **502**, 359 (2013).

[16] M. Adachi, Y. Kousaka, and K. Okuyama, J. Aerosol Sci **16**, 109 (1985).

[17] K. Nagato, Int. J. Mass spectrom. **285**, 12 (2009).

[18] K. Nagato and M. Nakauchi, J. Chem. Phys. **141**, 164309 (2014).

[19] J. H. Seinfeld and S. N. Pandis, *Atmospheric Chemistry and Physcs: From Air Pollution to Climate Change* (Wiley-Interscience, 2006), 2nd edn.

[20] N. Bork, T. Kurtén, M. B. Enghoff, J. O. P. Pedersen, K. V. Mikkelsen, and H. Svensmark, Atmos. Chem. Phys. **12**, 3639 (2012).

[21] J. F. Ziegler, J. P. Biersack, and U. Littmark, *The Stopping and Range of Ions in Solids* (Pergamon Press, New York, 1985).

[22] C. Willis and A. W. Boyd, International Journal for Radiation Physics and Chemistry **8**,

71 (1976).

[23] R. Wilding and R. G. Harrison, Atmos. Environ. **39**, 5876 (2005).

[24] T. Seto, T. Nakamoto, K. Okuyama, M. Adachi, Y. Kuga, and K. Takeuchi, J. Aerosol Sci **28**, 193 (1997).

[25] Y. Kuga, M. Hirasawa, T. Seto, K. Okuyama, and K. Takeuchi, Applied Physics A-Materials Science & Processing **68**, 75 (1999).

[26] O. Möhler, T. Reiner, and F. Arnold, The Journal of Chemical Physics **97**, 8233 (1992).

[27] D. Salcedo *et al.*, Int. J. Mass spectrom. **231**, 17 (2004).

[28] W. R. Stockwell and J. G. Calvert, Atmos. Environ. **17**, 2231 (1983).

[29] T. Hakoda, A. Shimada, K. Matsumoto, and K. Hirota, Plasma Chem. Plasma Process. **29**, 69 (2009).

[30] P. Hvelplund, J. O. P. Pedersen, K. Støchkel, M. B. Enghoff, and T. Kurtén, Int. J. Mass spectrom. **341–342**, 1 (2013).

[31] H. Kobara, H. Yamauchi, K. Takeuchi, and T. Ibusuki, Chem. Lett. **29**, 848 (2000).

Figure captions

Fig.1 Schematic drawing of the experimental setup.

Fig.2 Dependence of SO_2 consumption on proton-beam current for the case where the humidity of the sample gas was 30% RH (filled square) and the SO_2 mixing ratio of 100 ppb. The SO_2 consumption for a humidity of 52% (open diamond) and 9% (open triangle) are also shown. Solid line shows the fitted curve with power of 0.67.

Fig.3 Dependence of SO_2 consumption on the SO_2 concentration. The proton beam current was 200 pA. Humidity of the sample gas was 30%.

Fig.4 Mobility distributions of positively charged (solid line) and negatively charged droplets (dotted line) produced by proton beam of 200 pA. The sample gas was a mixture of $N_2/H_2O/SO_2$, with SO_2 concentrations of 150 ppb (black), 100 ppb (red), 50 ppb (green) and 20 ppb (blue). The humidity of the sample gas was 30%.

Fig.5 Mobility distributions of positively charged droplets produced by corona discharge in a mixture gas of $N_2/H_2O/SO_2$, with a SO_2 concentrations of 200 ppb (black), 150 ppb (red), 100 ppb (green) and 50 ppb (blue). The discharge current was 4.0 μA, and the humidity was 30%.

Fig. 6 Particle-flow rates of positively charged droplets are shown as a function of SO_2 consumption. The data were taken with different beam intensities (crosses), and SO_2 concentrations (circles). The triangle is a particle-flow rate for the

measurement using N_2/H_2O gas with 73% RH. The dashed curve corresponds to the fitted curve using a functional form of $R = \alpha S^{\beta}$ (R: particle flow rate, S: SO_2 consumption, see text).

Fig. 7 Dependence of the volume-yield rate (see text) of produced droplets on the amount of SO_2 consumption. The consumptions were changed by controlling beam intensity (crosses) and the concentration of SO_2 (circles). The triangle shows a volume-yield rate for the measurement using N_2/H_2O gas with 73% RH. The dashed line is a result of linear fit using $V = aS$ (V: volume-yield rate, S: SO_2 consumption, see text).

Figures

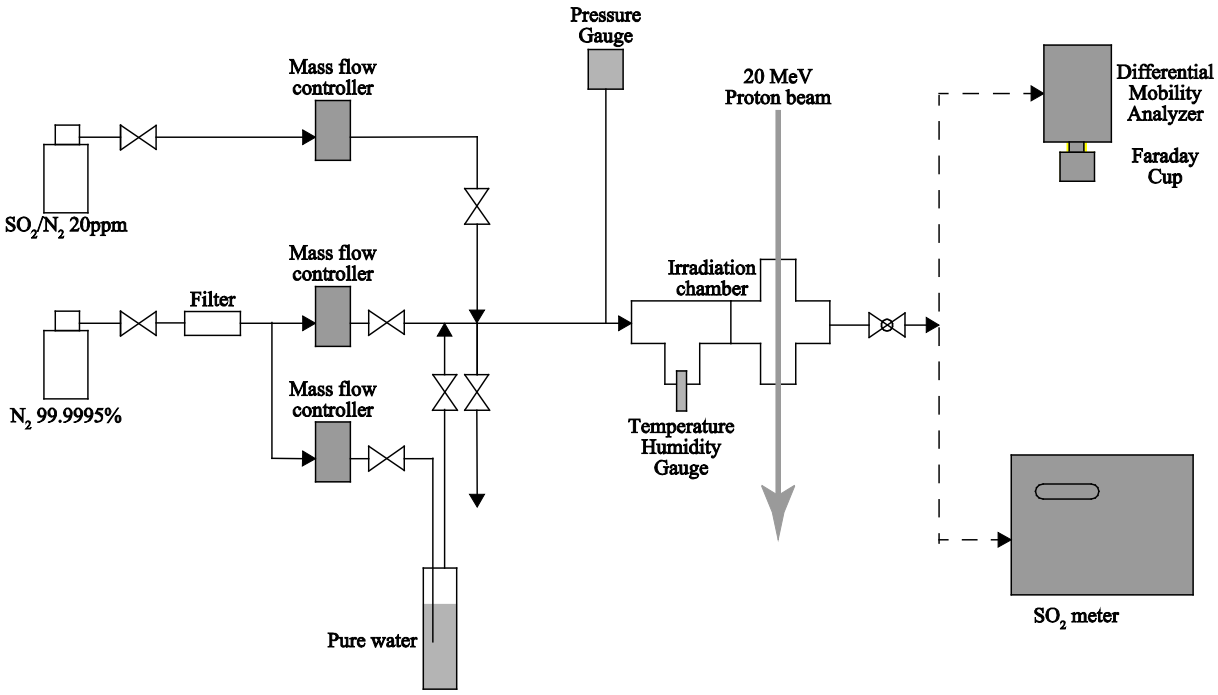

Fig. 1

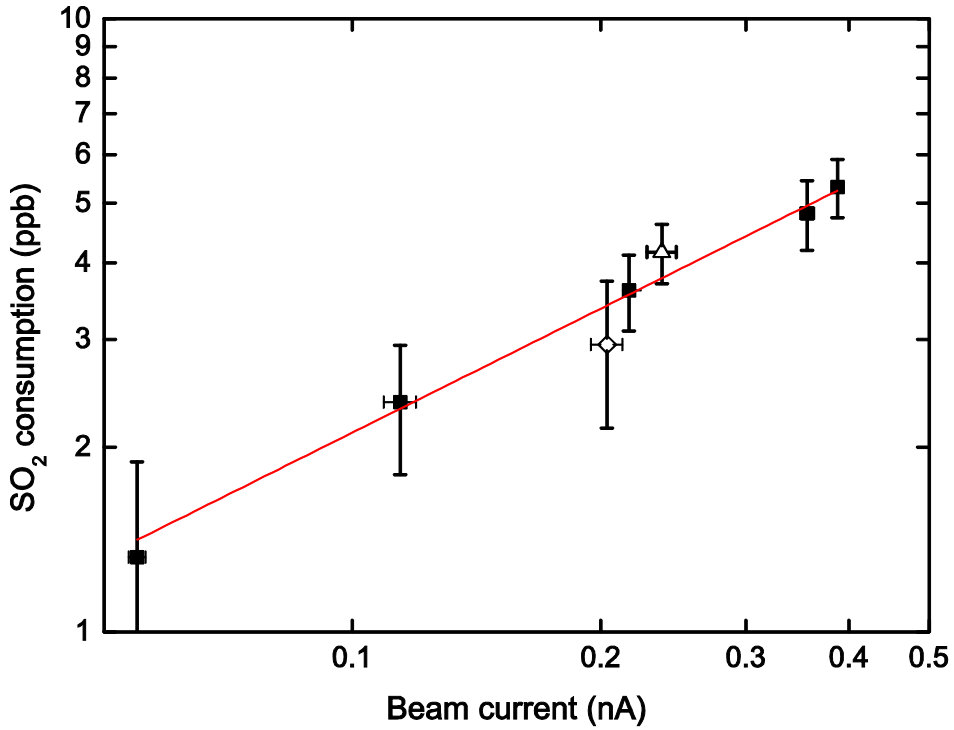
10
9
8
7
6
5
4
3
2
1
SO2 consumption (ppb)
0.1
0.2
0.3
0.4
0.5
Beam current (nA)

Fig. 2

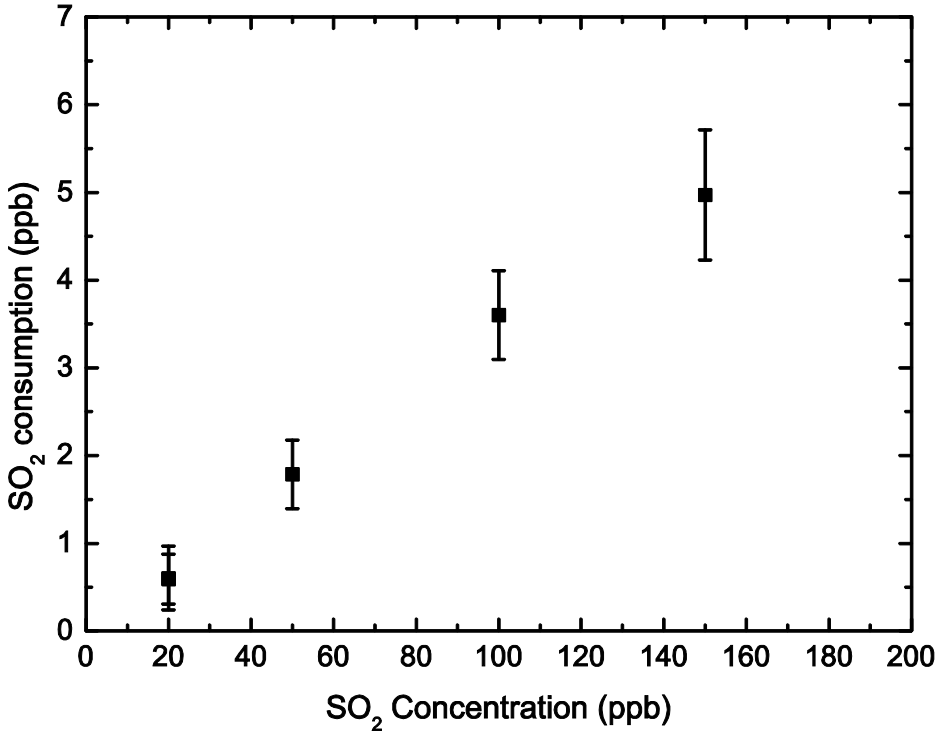
SO2 consumption (ppb)
SO2 Concentration (ppb)
0
1
2
3
4
5
6
7
0
20
40
60
80
100
120
140
160
180
200

Fig. 3

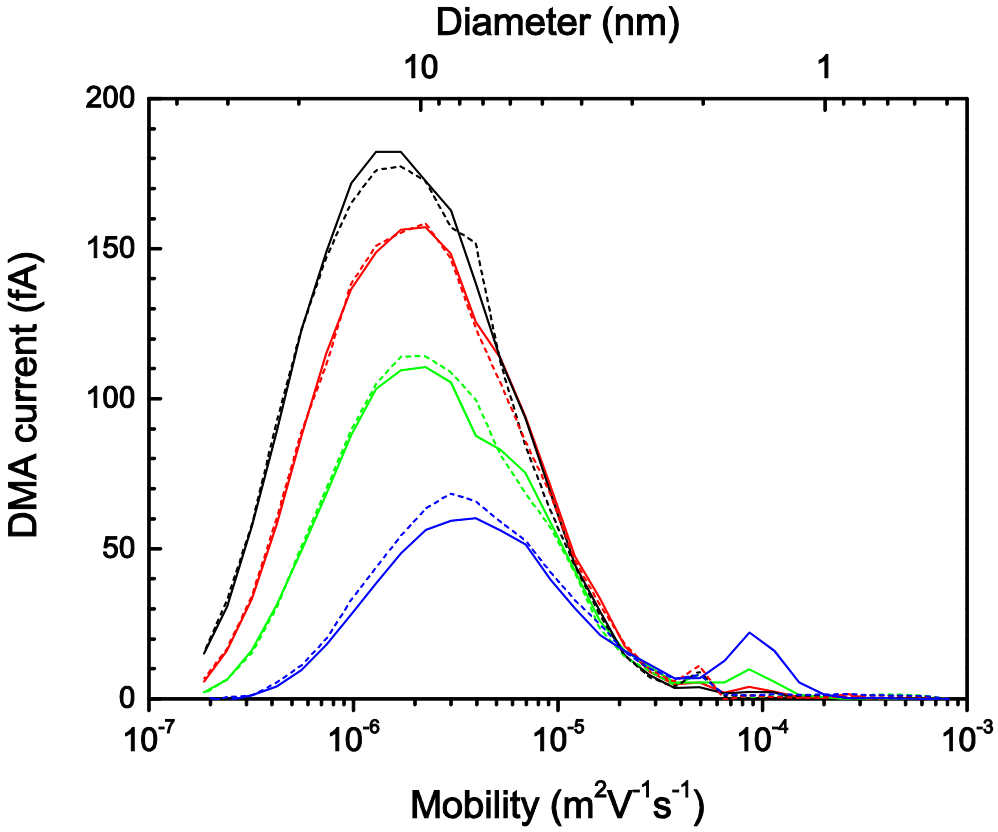
Diameter (nm)
10
1
200
150
100
50
0
DMA current (fA)
10^-7
10^-6
10^-5
10^-4
10^-3
Mobility (m^2V^-1s^-1)

Fig. 4

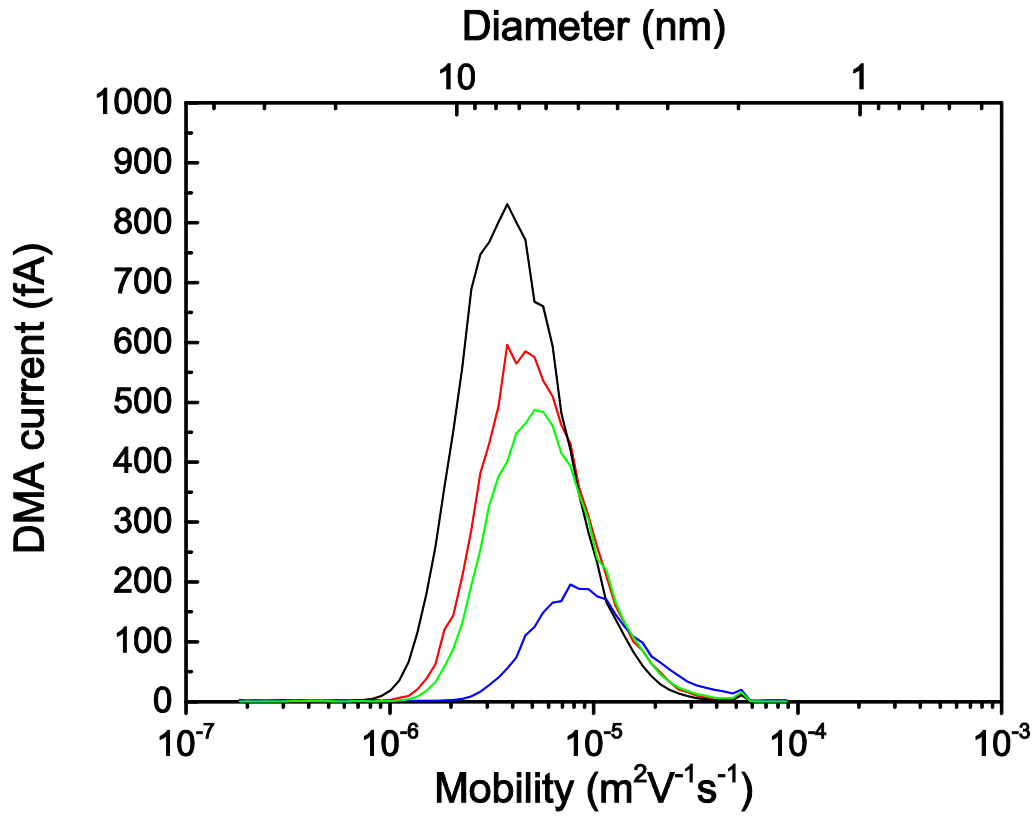
Diameter (nm)
10
1
1000
900
800
700
600
500
400
300
200
100
0
DMA current (fA)
10-7
10-6
10-5
10-4
10-3
Mobility (m2V-1s-1)

Fig. 5

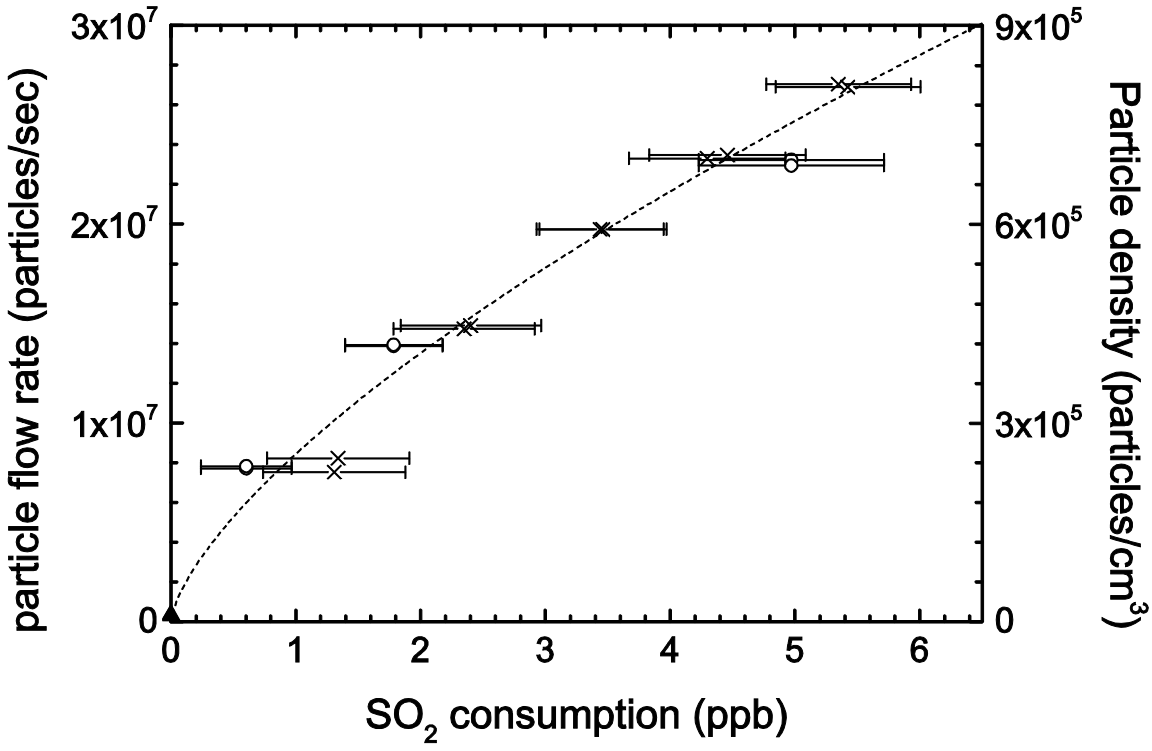
3x10^7
2x10^7
1x10^7
0
particle flow rate (particles/sec)
9x10^5
6x10^5
3x10^5
0
Particle density (particles/cm^3)
0
1
2
3
4
5
6
SO2 consumption (ppb)

Fig. 6

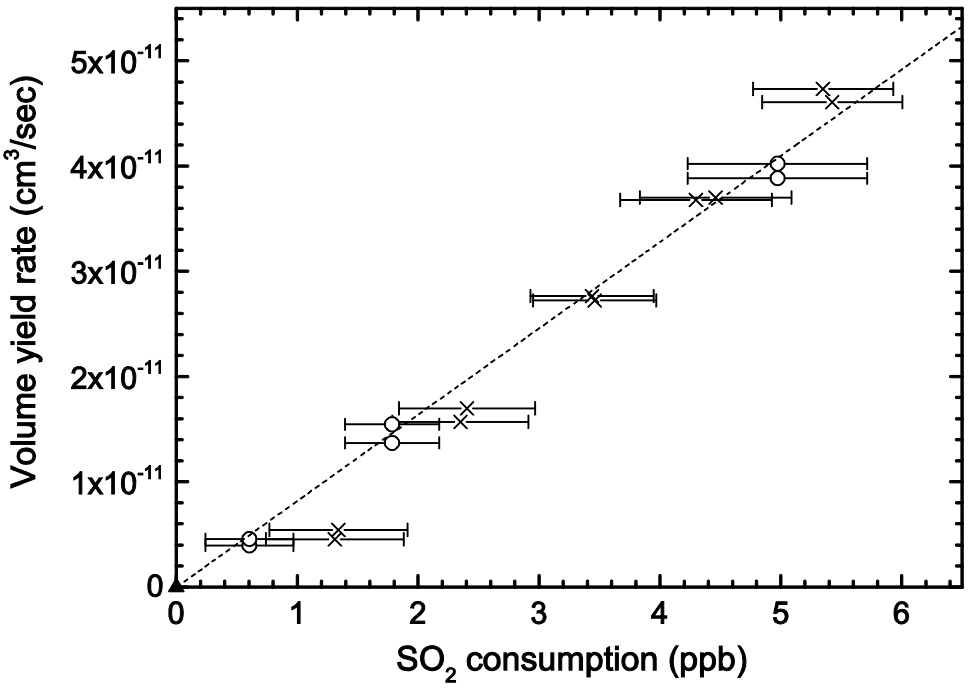
Volume yield rate (cm³/sec)
5x10⁻¹¹
4x10⁻¹¹
3x10⁻¹¹
2x10⁻¹¹
1x10⁻¹¹
0
0
1
2
3
4
5
6
SO₂ consumption (ppb)

Fig. 7